

Waiting times, probabilities and the Q factor of fluorescent photons

Henk F. Arnoldus* and Robertsen A. Riehle

Department of Physics and Astronomy, Mississippi State University,
P.O. Drawer 5167, Mississippi State, Mississippi, 39762-5167, USA

(Received 30 April 2012; final version received 9 May 2012)

Photons in resonance fluorescence from a single atom are correlated, and this affects the photon detection statistics. We consider the time dependence of the variance for the number of counts in a time interval $[0, T]$, and we show that there exist Poisson points for certain values of the atomic parameters. At these points, the variance equals the average, like for a Poisson process. We also show that the conditional probability density for the detection of the n th photon after a detection of a photon at time zero can be obtained from the conditional probability density for the first photon, and we illustrate this by computing several conditional probability densities for a special case of interest. The unconditional probability density for the detection of the n th photon can be obtained from the conditional probability densities and the probability for detecting n photons in $[0, T]$ can subsequently be found from the unconditional probability densities.

Keywords: photon statistics; resonance fluorescence; Q factor; sub-Poisson statistics; antibunching

1. Introduction

When light is detected by a photomultiplier tube, the recorded photoelectron pulses are interpreted as observations of photons, which are absorbed from the incoming light by the detector. Photon counts are considered as events (dots) on the time axis, and these events are highly random due to the quantum mechanical nature of the detection process (photo-excitation of atoms in the detector), and also possibly due to randomness in the light to be detected. If the light can be represented by a classical electric field $E(t)$, at the location of the detector, then this field will in general have stochastic fluctuations, for instance if it is emitted by a large number of atoms, like in a gas discharge or a filament source. Certain types of radiation require a quantum description, in which case $E(t)$ is an operator field, and additional randomness possibly enters the distribution of photon events due to inherent quantum uncertainties.

When light is observed through photon counting, properties of the radiation are reflected in the correlations in arrival times of photons, and in the statistical distribution of the photon events. The most comprehensive account of the statistical properties of random events is by means of the intensity

correlations, defined as [1]

$$I_k(t_1, t_2, \dots, t_k) dt_1 dt_2 \dots dt_k \\ = \text{probability for an event in } [t_1, t_1 + dt_1], \text{ and } \dots \text{ and} \\ \text{an event in } [t_k, t_k + dt_k], \text{ irrespective of events at} \\ \text{other times, and with } t_1 < t_2 < \dots < t_k, \quad (1)$$

for $k = 1, 2, \dots$. In the theory of random events, these functions are usually referred to as distribution functions [2]. The relation between the incident field on the detector and the counting statistics is given by [3,4]

$$I_k(t_1, t_2, \dots, t_k) \\ = \zeta^k \langle E(t_1)^{(-)} \dots E(t_k)^{(-)} E(t_k)^{(+)} \dots E(t_1)^{(+)} \rangle, \quad (2)$$

where $E(t)$ is $E(t)$, projected on a polarization direction, and $(+)$ and $(-)$ indicate the positive and negative frequency parts of $E(t)$, respectively. Parameter ζ is an overall constant, which depends on the detector aperture, the detector volume, etc, and $\langle \dots \rangle$ indicates an average over either stochastic fluctuations in the radiation field or a quantum average, depending on the type of radiation to be detected.

We shall consider the radiation emitted by a two-state atom in a laser beam, e.g., resonance fluorescence. This elementary system has been studied extensively, both experimentally and theoretically.

*Corresponding author. Email: hfa1@msstate.edu

The two-photon correlation function $I_2(t_1, t_2)$ vanishes for $t_2 = t_1$, a phenomenon called antibunching. This is a result of the fact that after the emission of the first photon at time t_1 , the atom is in the ground state, and it takes a finite time for the atom to reach the excited state again, after which the second photon can be emitted. This has been verified experimentally [5–7]. It can be shown [8] that for classical radiation we have $I_2(t_1, t_1) \geq I(t_1)^2$, and therefore antibunching is considered evidence for the quantum nature of resonance fluorescence. Another feature of fluorescence is that the variance of the count statistics may be smaller than the average. Such sub-Poisson statistics is prohibited for classical radiation [9], and its observation [10–14] is further evidence that resonance fluorescence radiation has no classical description.

There are numerous other statistical properties of random events that have not received much attention for fluorescence radiation. Most notably, the probabilities $P_n(T)$ for detecting n photons in a time interval $[0, T]$ and the probability densities for the detection or emission of photons have rarely been considered. We shall show that these properties of the radiation can be obtained for resonance fluorescence, and we present specific results for particular cases of interest.

2. Random events and the Q factor

Let $P_n(T)$ be the probability for observing n events in a counting time interval $[0, T]$. The factorial moments of the random events in $[0, T]$ are defined as

$$S_k(T) = \sum_{n=k}^{\infty} \frac{n!}{(n-k)!} P_n(T), \quad k = 0, 1, 2, \dots \quad (3)$$

This relation can be inverted as

$$P_n(T) = \frac{(-1)^n}{n!} \sum_{k=n}^{\infty} \frac{(-1)^k}{(k-n)!} S_k(T), \quad (4)$$

as can be checked by inspection. The factorial moments are determined by the intensity correlations as [1]

$$S_k(T) = k! \int_0^T dt_k \int_0^{t_k} dt_{k-1} \dots \int_0^{t_2} dt_1 I_k(t_1, \dots, t_k), \quad k = 1, 2, \dots, \quad (5)$$

and $S_0(T) = 1$. For the detection of radiation, the intensity correlations are given by Equation (2), and therefore Equations (5) and (4) give the factorial moments and the probabilities.

The average number of events in $[0, T]$ is

$$\mu(T) = \sum_{n=0}^{\infty} n P_n(T) = S_1(T) = \int_0^T dt_1 I_1(t_1), \quad (6)$$

and the variance is

$$\begin{aligned} \sigma(T)^2 &= \sum_{n=0}^{\infty} (n - \mu(T))^2 P_n(T) \\ &= S_2(T) - S_1(T)^2 + S_1(T). \end{aligned} \quad (7)$$

For independent events, $P_n(T)$ is a Poisson distribution, and $\sigma(T)^2 = \mu(T)$. A convenient measure for the deviation from Poisson statistics is Mandel's Q factor

$$Q(T) = \frac{\sigma(T)^2 - \mu(T)}{\mu(T)}, \quad (8)$$

which can also be expressed as

$$Q(T) = \frac{S_2(T) - S_1(T)^2}{S_1(T)}. \quad (9)$$

Clearly, we have $Q(T) \geq -1$. For $-1 \leq Q(T) < 0$ we have $\sigma(T)^2 < \mu(T)$, and the statistics is said to be sub-Poissonian, and for $Q(T) > 0$ the statistics is super-Poissonian.

We shall consider stationary distributions of random events. Then the intensity correlations $I_k(t_1, \dots, t_k)$ can only depend on the time arguments through the time differences. In particular, $I_1(t_1)$ is independent of t_1 , and we shall simply write I . This I is referred to as the intensity of the random process. The average for a stationary process is $\mu(T) = IT$. For the two-time correlation function we have $I_2(t_1, t_2) = I_2(0, t_2 - t_1)$. When we introduce the normalized correlation function

$$\kappa(\tau) = \frac{I_2(0, \tau)}{I^2} - 1, \quad (10)$$

then the Q factor can be represented as

$$Q(T) = 2I \int_0^T d\tau \left(1 - \frac{\tau}{T}\right) \kappa(\tau). \quad (11)$$

When we expand the right-hand side in a Taylor series for T small, we find

$$Q(T) = IT\kappa(0) + O(T^2). \quad (12)$$

Therefore, for small counting times the sign of $Q(T)$ is the same as the sign of $\kappa(0)$. For resonance fluorescence we have $I_2(0, 0) = 0$ (ultimate antibunching), so $\kappa(0) = -1$ and the statistics is sub-Poissonian. For long counting times we find

$$Q(\infty) = 2I \int_0^{\infty} d\tau \kappa(\tau), \quad (13)$$

provided that the integral over $\tau \kappa(\tau)$ is finite. In terms of the Laplace transform

$$\tilde{\kappa}(s) = \int_0^\infty d\tau e^{-s\tau} \kappa(\tau), \tag{14}$$

we then have

$$Q(\infty) = 2I\tilde{\kappa}(0). \tag{15}$$

Equation (13) expresses that $Q(\infty) < 0$ if the events are anti-bunched ($\kappa(\tau) < 0$) on average.

3. Event probability densities

The probability density for the appearance of the n th event is defined as

$$w_n(t)dt = \text{probability that the } n\text{th event appears in } [t, t + dt], \tag{16}$$

for $n = 1, 2, \dots$. It is shown in the Appendix that these probability densities can be expressed in terms of the probabilities as

$$w_n(t) = -\frac{d}{dt} \sum_{m=0}^{n-1} P_m(t). \tag{17}$$

The inverse of this relation is

$$P_0(T) = 1 - \int_0^T dt w_1(t), \tag{18}$$

$$P_n(T) = \int_0^T dt [w_n(t) - w_{n+1}(t)], \quad n = 1, 2, \dots, \tag{19}$$

as is most easily seen from Equations (A3) and (A4), and using $P_n(0) = \delta_{n0}$. Therefore, the probabilities and the probability densities determine each other uniquely. With Equation (4), the probability densities can also be expressed in terms of the factorial moments as

$$w_n(t) = \frac{(-1)^n}{(n-1)!} \sum_{k=n}^\infty \frac{(-1)^k}{k} \frac{1}{(k-n)!} \frac{d}{dt} S_k(t), \tag{20}$$

with inverse

$$S_k(T) = k \sum_{n=k}^\infty \frac{(n-1)!}{(n-k)!} \int_0^T dt w_n(t). \tag{21}$$

When we integrate Equation (17) over $[0, T]$ we find

$$\int_0^T dt w_n(t) = 1 - \sum_{m=0}^{n-1} P_m(T). \tag{22}$$

If $w_n(t)$ is to be a probability density, then it should hold that

$$\int_0^\infty dt w_n(t) = 1. \tag{23}$$

From Equation (22) we see that this requires that $P_m(\infty) = 0$, for $m = 0, 1, \dots, n-1$. For an arbitrary random event process, this is not necessarily the case. For a stationary process, however, this always holds. We shall only consider stationary processes. Then, let us introduce the random variable τ_n as the arrival time of the n th event, after $t = 0$. The expectation value of τ_n is then

$$\langle \tau_n \rangle = \int_0^\infty dt t w_n(t), \tag{24}$$

which is the average waiting time for the n th event to appear. The variance in τ_n is

$$(\Delta\tau_n)^2 = \int_0^\infty dt (t - \langle \tau_n \rangle)^2 w_n(t). \tag{25}$$

The function $w_n(t)$ is the probability density for the appearance of the n th event after a random initial time $t = 0$. A different type of distribution is the conditional probability density for the appearance of the n th event:

$$w_n(t|0)dt = \text{probability that the } n\text{th event appears in } [t, t + dt], \text{ after an event in } [-dt, 0]. \tag{26}$$

It is shown in the Appendix that for a stationary process the conditional probability densities can be found from the unconditional probability densities as

$$w_n(t|0) = -\frac{1}{I} \frac{d}{dt} \sum_{m=1}^n w_m(t), \tag{27}$$

where I is the intensity of the process. The inverse relation is

$$w_1(t) = w_1(0) - I \int_0^t dt' w_1(t'|0), \tag{28}$$

$$w_n(t) = w_n(0) - I \int_0^t dt' [w_n(t'|0) - w_{n-1}(t'|0)], \quad n = 2, 3, \dots \tag{29}$$

The conditional probability densities satisfy the normalization

$$\int_0^\infty dt w_n(t|0) = 1, \tag{30}$$

and the conditional waiting time for the n th event is

$$\langle \tau_n|0 \rangle = \int_0^\infty dt t w_n(t|0), \tag{31}$$

with variance

$$(\Delta\tau_n|0)^2 = \int_0^\infty dt(t - \langle\tau_n|0\rangle)^2 w_n(t|0). \quad (32)$$

4. Intensity correlations of resonance fluorescence

We shall consider a two-state atom, with the excited state $|e\rangle$ and the ground state $|g\rangle$ separated by an energy $\hbar\omega_o$, and electric dipole moment operator $\boldsymbol{\mu}$. The atom is irradiated by a monochromatic CW laser with angular frequency ω_L , amplitude E_o and polarization $\boldsymbol{\varepsilon}_L$. The detuning between the laser frequency and the atomic resonance is

$$\Delta = \omega_L - \omega_o, \quad (33)$$

and the complex Rabi frequency is

$$\Omega = \frac{E_o}{\hbar} \langle e | \boldsymbol{\mu} \cdot \boldsymbol{\varepsilon}_L | g \rangle. \quad (34)$$

The inverse lifetime of the excited state is the Einstein A coefficient of the transition. Fluorescence radiation will be emitted in spontaneous transitions from the excited state to the ground state as electric dipole radiation.

The intensity correlations of the emitted fluorescence have the form [14,15]

$$I_1(t_1) = \alpha A n_e(t_1), \quad (35)$$

$$I_k(t_1, \dots, t_k) = (\alpha A)^k f(t_k - t_{k-1}) \cdots f(t_2 - t_1) n_e(t_1), \quad (36)$$

$$k = 2, 3, \dots$$

Here, $n_e(t_1)$ is the population of $|e\rangle$ at time t_1 , and $f(t)$ is the population of $|e\rangle$ at time t , under the condition that the atom is in $|g\rangle$ at $t=0$. The constant α includes the constant ζ from Equation (2) and other overall factors of the dipole radiation. The retardation due to the travel time of the photons from the atom to the detector has been suppressed, since this only gives an overall time shift. The number of emitted photons per second at time t by a two-state atom is $An_e(t)$, and therefore we can interpret α as the probability that an emitted photon is detected. Equation (36) then has the following interpretation: the first photon is detected at time t_1 . Then the state of the atom evolves freely up to time t_2 , and then the second photon is detected. After the detection, the atom is in the ground state. Then it evolves freely again up to time t_3 , and the third photon is detected at time t_3 , and so on. Clearly, $f(0)=0$, which is the celebrated antibunching in resonance fluorescence.

The intensity correlations are determined by the function $f(t)$. Its Laplace transform is found to be

$$\tilde{f}(s) = \frac{\Omega_o^2}{2s} \frac{\frac{1}{2}A + s}{(A + s) \left[\left(\frac{1}{2}A + s \right)^2 + \Delta^2 \right] + \left(\frac{1}{2}A + s \right) \Omega_o^2}, \quad (37)$$

where $\Omega_o = |\Omega|$. Due to spontaneous decay, the atom will relax to a steady state on a time scale of $1/A$, and we shall assume that at $t=0$, the initial time for the photon counting, the atom is in its steady state. Then $n_e(t_1)$ in Equations (35) and (36) becomes $n_e(\infty)$, and we shall indicate this steady-state value by \bar{n}_e . Obviously, this is the same as $f(\infty)$, so we have

$$\bar{n}_e = f(\infty) = \lim_{s \rightarrow 0} s \tilde{f}(s), \quad (38)$$

and we obtain

$$\bar{n}_e = \frac{\Omega_o^2}{A^2 + 4\Delta^2 + 2\Omega_o^2}. \quad (39)$$

The behavior of $f(t)$ for t small can be found by considering $s \rightarrow \infty$ in $\tilde{f}(s)$. We find $f(0) = f'(0) = 0$, and $f''(0) = \Omega_o^2/2$. Therefore,

$$f(t) = \frac{1}{4} \Omega_o^2 t^2 + O(t^3), \quad (40)$$

for t small.

The function $f(t)$ determines the photon statistics of resonance fluorescence. It depends on the parameters Ω_o , Δ and A . We shall use $1/A$ as the unit of time, e.g. we set $\hat{t} = At$ and $\hat{T} = AT$, and A as the unit of frequency, so we set $\hat{\Omega}_o = \Omega_o/A$ and $\hat{\Delta} = \Delta/A$. In this fashion, only $\hat{\Omega}_o$ and $\hat{\Delta}$ appear as free parameters in the problem. Finding $f(t)$ by Laplace inverse of the right-hand side of Equation (37) requires factoring a 3rd degree polynomial. Although this can be done, the result is not very appealing. The most important special case of interest is resonance ($\Delta = 0$), for which [16]

$$f(t) = \bar{n}_e \left\{ 1 - e^{-\frac{3}{4}\hat{t}} \left[\frac{3}{\rho_1} \sinh\left(\frac{1}{4}\rho_1\hat{t}\right) + \cosh\left(\frac{1}{4}\rho_1\hat{t}\right) \right] \right\}, \quad (41)$$

with

$$\rho_1 = \sqrt{1 - 16\hat{\Omega}_o^2}. \quad (42)$$

For $\hat{\Omega}_o > 1/4$, ρ_1 is positive imaginary, and the hyperbolic functions become trigonometric functions. Figure 1 illustrates the behavior of $f(t)$ for various values of $\hat{\Omega}_o$. The function is monotonically increasing for $\hat{\Omega}_o$ small, and for $\hat{\Omega}_o$ large we see Rabi oscillations. For the off-resonance case, $f(t)$ can be found easily for $\hat{\Omega}_o^2 = 2\hat{\Delta}^2 + 1/18$, and here we see $\hat{\Delta}$ as the free parameter. We find

$$f(t) = \bar{n}_e \left\{ 1 - \frac{4}{9\rho_2^2} e^{-\frac{2}{3}\hat{t}} \left[\frac{1}{3} - \frac{3}{4}\rho_2^2 + \left(3\rho_2^2 - \frac{1}{3} \right) \cosh(\rho_2\hat{t}) + \frac{3}{2}\rho_2 \sinh(\rho_2\hat{t}) \right] \right\}, \quad (43)$$

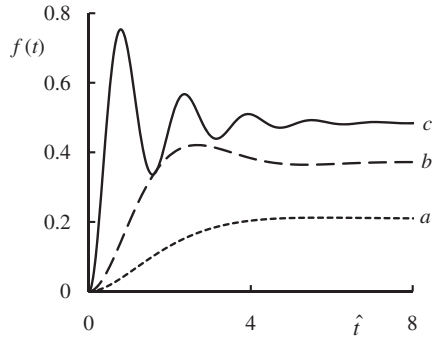


Figure 1. Graphs of $f(t)$ for $\Delta = 0$. For curves a , b and c we have $\hat{\Omega}_0 = 0.6, 1.2$ and 4 , respectively.

with

$$\rho_2 = \sqrt{\frac{1}{36} - 3\hat{\Delta}^2}. \quad (44)$$

The behavior of $f(t)$ is very similar as in Figure 1, with Rabi oscillations setting in for $|\hat{\Delta}|$ large.

5. The Q factor and Poisson points

For resonance fluorescence we have

$$I_2(0, \tau) = \alpha A f(\tau) I, \quad (45)$$

with $I = \alpha A \bar{n}_e$. The function $\kappa(\tau)$ from Equation (10) becomes

$$\kappa(\tau) = \frac{f(\tau)}{\bar{n}_e} - 1, \quad (46)$$

and therefore $Q(T)$, Equation (11), is determined by $f(\tau)$. With Equation (40) we find

$$\kappa(\tau) = -1 + \frac{1}{4\bar{n}_e} \Omega_0^2 \tau^2 + O(\tau^3), \quad (47)$$

for τ small, and so the Q factor becomes

$$Q(T) = -IT + \frac{1}{24} \alpha A \Omega_0^2 T^3 + O(T^4), \quad (48)$$

for small T . Therefore, for small counting times T , the statistics is always sub-Poissonian, and this is an immediate consequence of the antibunching.

From Equations (46) and (37) we find for the Laplace transform of $\kappa(\tau)$

$$\tilde{\kappa}(s) = \frac{\Delta^2 - (\frac{1}{2}A + s)(\frac{3}{2}A + s)}{(A + s)\left[\left(\frac{1}{2}A + s\right)^2 + \Delta^2\right] + (\frac{1}{2}A + s)\Omega_0^2}. \quad (49)$$

Since the Laplace transform of $\tau\kappa(\tau)$ is $-\tilde{\kappa}'(s)$, we have

$$\int_0^\infty d\tau \tau \kappa(\tau) = -\tilde{\kappa}'(0), \quad (50)$$

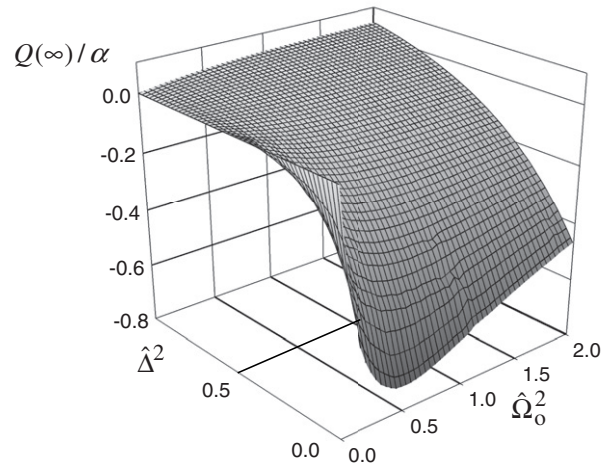


Figure 2. A graph of $Q(\infty)/\alpha$, given by Equation (50), as a function of $\hat{\Omega}_0^2$ and $\hat{\Delta}^2$.

and this is finite, as can be seen from Equation (49). Therefore, $Q(\infty) = 2I\tilde{\kappa}(0)$, and we find

$$Q(\infty) = \frac{1}{2} \alpha \hat{\Omega}_0^2 \frac{\hat{\Delta}^2 - \frac{3}{4}}{(\frac{1}{2}\hat{\Omega}_0^2 + \hat{\Delta}^2 + \frac{1}{4})^2}, \quad (51)$$

a well-known result [17]. For $|\hat{\Delta}| < \sqrt{3}/2$ the statistics is sub-Poissonian, and for $|\hat{\Delta}| > \sqrt{3}/2$ the statistics is super-Poissonian for long counting times. The minimum value of $Q(\infty)$ is $-3\alpha/4$, which occurs for $\hat{\Delta} = 0$, $\hat{\Omega}_0 = 1/\sqrt{2}$. Figure 2 shows $Q(\infty)/\alpha$ as a function of $\hat{\Omega}_0^2$ and $\hat{\Delta}^2$.

For $\Delta = 0$ the function $Q(T)$ is found to be

$$Q(T) = Q(\infty) + \frac{2\alpha\bar{n}_e}{\hat{T}} Z(T), \quad (52)$$

with

$$Z(T) = \frac{1}{4(1 + 2\hat{\Omega}_0^2)^2} \left\{ 27 + \rho_1^2 - e^{-\frac{3}{4}\hat{T}} \left[(27 + \rho_1^2) \cosh\left(\frac{1}{4}\rho_1\hat{T}\right) + \frac{9}{\rho_1} (3 + \rho_1^2) \sinh\left(\frac{1}{4}\rho_1\hat{T}\right) \right] \right\}, \quad (53)$$

and with $Q(\infty)$ and \bar{n}_e from Equations (51) and (39), respectively (with Δ set to zero). Figures 3 and 4 show $Q(T)/\alpha$ for several values of $\hat{\Omega}_0$. For small values of $\hat{\Omega}_0$, the Q factor decreases monotonically from zero at $\hat{T} = 0$ to its steady-state value given by Equation (51), as shown in Figure 3. For curve c we have $\hat{\Omega}_0 = 1/\sqrt{2}$, and this corresponds to the lowest possible value of $Q(\infty)/\alpha$, which is $-3/4$. The function $f(t)$ from Equation (41) approaches its asymptotic value $f(\infty)$ exponentially, but the corresponding function $Q(T)$ approaches $Q(\infty)$ as $O(1/T)$. For larger values of $\hat{\Omega}_0$,

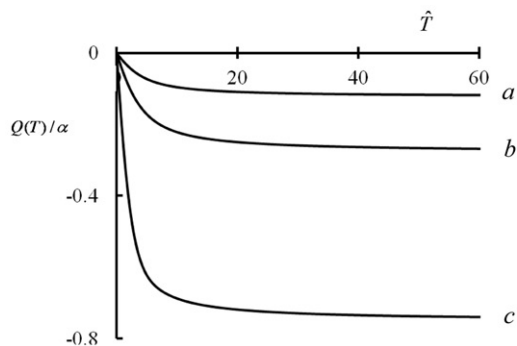


Figure 3. Three graphs of $Q(T)/\alpha$ for $\Delta = 0$. Curves a , b and c correspond to $\hat{\Omega}_0 = 0.15, 0.24$ and $1/\sqrt{2}$, respectively.

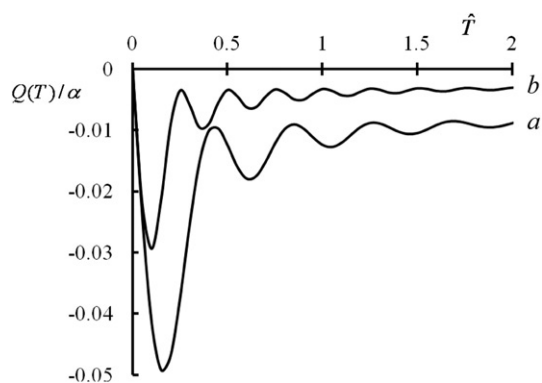


Figure 4. Curves a and b are graphs of $Q(T)/\alpha$ for $\Delta = 0$, with $\hat{\Omega}_0 = 15$ and 25 , respectively.

as in Figure 4, $Q(\infty)/\alpha$ has a sharp minimum for a small value of \hat{T} , after which $Q(T)/\alpha$ increases and then approaches a small negative $Q(\infty)/\alpha$. We also note that oscillations appear, but the curves never cross the \hat{T} axis, and therefore the statistics is sub-Poissonian for all \hat{T} .

Let us now consider the case $\hat{\Omega}_0^2 = 2\hat{\Delta}^2 + 1/18$. The function $Q(T)$ has again the form of Equation (52), but here we have

$$\begin{aligned}
 Z(T) = & \frac{1}{12\rho_2^2} (4 - 9\rho_2^2)(1 - e^{-\frac{2}{3}\hat{T}}) \\
 & + \frac{64}{\rho_2^2(5 + 36\hat{\Delta}^2)^2} \left\{ 3\rho_2^2(1 + \rho_2^2) - \frac{4}{27} \right. \\
 & - e^{-\frac{2}{3}\hat{T}} \left\{ \left[3\rho_2^2(1 + \rho_2^2) - \frac{4}{27} \right] \cosh(\rho_2\hat{T}) \right. \\
 & \left. \left. + \rho_2 \left(\frac{2}{9} + \frac{11}{2}\rho_2^2 \right) \sinh(\rho_2\hat{T}) \right\} \right\}. \quad (54)
 \end{aligned}$$

Figure 5 shows graphs of $Q(\infty)/\alpha$ for various values of $\hat{\Delta}$. For small values of $\hat{\Delta}$, as for curve a , the function

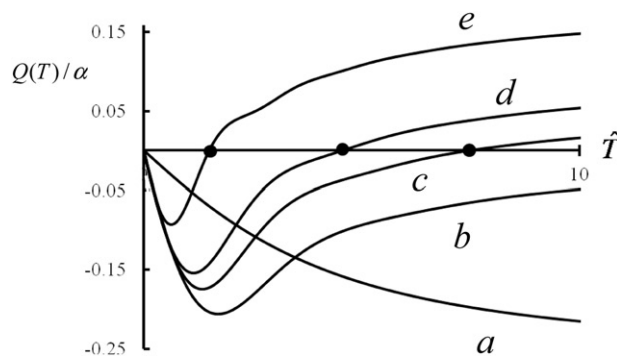


Figure 5. Graphs of $Q(T)/\alpha$ as a function of \hat{T} for the case $\hat{\Omega}_0^2 = 2\hat{\Delta}^2 + 1/18$. For curves a, b, c, d and e the values of $\hat{\Delta}$ are $0, \sqrt{3}/2, 1.05, 1.2$ and 2 , respectively.

$Q(T)/\alpha$ decreases monotonically from zero to its negative long-time value $Q(\infty)/\alpha$. For larger $\hat{\Delta}$, the value of $Q(\infty)/\alpha$ is larger, and the curve has a minimum. For curve b we have $\hat{\Delta} = \sqrt{3}/2$ and $Q(\infty)/\alpha = 0$. For larger $\hat{\Delta}$, $Q(\infty)/\alpha$ is positive, so the curve has to cross the \hat{T} axis, and these points are indicated by black dots. At these ‘Poisson points’, the variance of the counting distribution equals the average. Obviously, such a Poisson point exists for $|\hat{\Delta}| > \sqrt{3}/2$, because then $Q(\infty)/\alpha$ is positive, whereas for small \hat{T} it is negative. The function $Q(T)$ is determined by $f(t)$, and this function has large Rabi oscillations when $\hat{\Omega}_0$ or $|\hat{\Delta}|$ is large, as can be seen from Figure 1. However, the oscillations in the function $Q(T)$ are very small, as in Figure 4, and they do not result in a crossing of the \hat{T} axis, so they do not lead to additional Poisson points.

It appears, in general, that there is one Poisson point T_P for $|\hat{\Delta}| > \sqrt{3}/2$, and none for $|\hat{\Delta}| < \sqrt{3}/2$. This conclusion holds for the two cases considered above. In order to strengthen this conjecture, let us consider one more case of interest. In the weak field limit, $\hat{\Omega}_0 \ll 1$, we have

$$\kappa(\tau) = e^{-A\tau} - 2 \cos(\Delta\tau) e^{-\frac{1}{2}A\tau}. \quad (55)$$

The function $Q(T)$ has the form of Equation (52), and here we have

$$\begin{aligned}
 Z(T) = & e^{-\hat{T}} - 1 + \frac{2}{(\hat{\Delta}^2 + \frac{1}{4})^2} \left\{ \left(\frac{1}{4} - \hat{\Delta}^2 \right) \left[1 - \cos(\hat{\Delta}\hat{T}) e^{-\frac{1}{2}\hat{T}} \right] \right. \\
 & \left. + \hat{\Delta} \sin(\hat{\Delta}\hat{T}) e^{-\frac{1}{2}\hat{T}} \right\}. \quad (56)
 \end{aligned}$$

Figure 6 shows several graphs of $Q(T)$, and we see indeed that there is one Poisson point for $|\hat{\Delta}| > \sqrt{3}/2$. The value $Q(\infty)$ is zero for $|\hat{\Delta}| = \sqrt{3}/2$ and for $|\hat{\Delta}| \rightarrow \infty$, and is maximum for $|\hat{\Delta}| = \sqrt{7}/2$. For curve

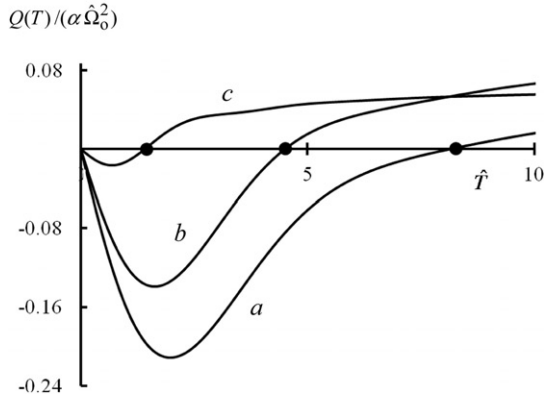


Figure 6. Three graphs of the Q factor as a function of \hat{T} in the weak field limit. For curves a , b , and c we have $\hat{\Delta} = 1.03$, 1.2 and 2.5 , respectively. The Poisson points are indicated by black dots. For $\hat{\Delta} < \sqrt{3}/2 = 0.866$, $Q(T)$ is negative for all \hat{T} and there are no Poisson points.

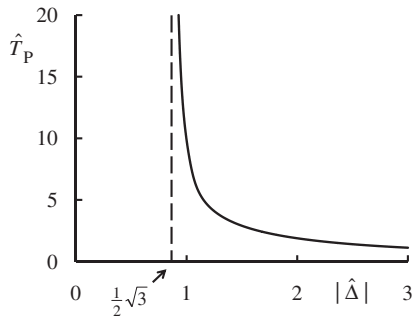


Figure 7. The dependence of the Poisson point \hat{T}_p on $|\hat{\Delta}|$ in the weak field limit. The dashed line is $|\hat{\Delta}| = \sqrt{3}/2$, and there are no solutions to the left of this line.

c in the figure, $Q(\infty)$ is smaller than for curve b , and that is why the curves cross. The location of the Poisson point can be found by numerically solving $Q(T_p) = 0$, given $|\hat{\Delta}|$, and the result is shown in Figure 7. We see that indeed there are no solutions for $|\hat{\Delta}| < \sqrt{3}/2$.

6. Statistical functions

The intensity correlations for resonance fluorescence are given by Equations (35) and (36) in terms of the function $f(t)$. When substituted into Equation (5), this determines the factorial moments of the count distribution as a function of the counting time T . Since the intensity correlations factor, the multiple integrals in Equation (5) are of the convolution type. We then find for the Laplace transforms (in T) of the factorial moments

$$\tilde{S}_0(s) = \frac{1}{s}, \tag{57}$$

$$\tilde{S}_k(s) = I \frac{k!}{s^2} [\alpha A \tilde{f}(s)]^{k-1}, \quad k = 1, 2, \dots \tag{58}$$

With Equation (4) we then find the Laplace transforms of the probabilities:

$$\tilde{P}_0(s) = \frac{1}{s} - \frac{I}{s^2} \frac{1}{1 + \alpha A \tilde{f}(s)}, \tag{59}$$

$$\tilde{P}_n(s) = \frac{I}{s^2} \frac{[\alpha A \tilde{f}(s)]^{n-1}}{[1 + \alpha A \tilde{f}(s)]^{n+1}}, \quad n = 1, 2, \dots \tag{60}$$

The probability densities follow from Equation (17), which can also be written as

$$w_n(t) = \frac{d}{dt} \sum_{m=n}^{\infty} P_m(t), \tag{61}$$

since the probabilities $P_n(T)$ add to unity. This gives

$$\tilde{w}_n(s) = s \sum_{m=n}^{\infty} \tilde{P}_m(s), \tag{62}$$

because $P_m(0) = 0$ for $m \geq 1$. With Equation (60) we then obtain

$$\tilde{w}_n(s) = \frac{I}{s} \frac{[\alpha A \tilde{f}(s)]^{n-1}}{[1 + \alpha A \tilde{f}(s)]^n}. \tag{63}$$

The value of $w_n(t)$ for $t \rightarrow 0$ can be found from

$$w_n(0) = \lim_{s \rightarrow \infty} s \tilde{w}_n(s), \tag{64}$$

and since $\tilde{f}(s)$ goes to zero for $s \rightarrow \infty$, we find

$$w_n(0) = I \delta_{n1}, \tag{65}$$

as could be expected. With Equation (27) we have for the conditional probability densities

$$\tilde{w}_n(s|0) = 1 - \frac{1}{I} \sum_{m=1}^n s \tilde{w}_m(s), \tag{66}$$

since $w_m(0) = I \delta_{m1}$. With Equation (63) this yields

$$\tilde{w}_n(s|0) = \left(\frac{\alpha A \tilde{f}(s)}{1 + \alpha A \tilde{f}(s)} \right)^n. \tag{67}$$

For $t = 0$ we find

$$w_n(0|0) = 0. \tag{68}$$

For $n = 1$ this is again the antibunching of two photons.

7. Average waiting time and variance

The function $w_n(t)$ is the probability density for the random variable τ_n , which is the arrival time of the

n th photon. With Equation (38) and $\alpha A\bar{n}_e = I$ we find from Equation (63) that $\tilde{w}_n(0) = 1$. In the time domain this is Equation (23), so this condition is fulfilled indeed. The waiting time for the n th photon, $\langle\tau_n\rangle$, is computed as in Equation (24). We use Equation (17) for $w_n(t)$, and integrate by parts. The integrated part is zero (it can be checked from the Laplace transform for $\tilde{P}_k(s)$ that $tP_k(t)$ vanishes for $t \rightarrow \infty$), and we obtain

$$\langle\tau_n\rangle = \sum_{m=0}^{n-1} \int_0^\infty dt P_m(t) = \sum_{m=0}^{n-1} \tilde{P}_m(0). \quad (69)$$

For $m=1, 2, \dots$, we find immediately $\tilde{P}_m(0) = 1/I$ from Equations (60) and (38). For $m=0$ we need to do this more carefully, since in Equation (59) we need to combine the two terms. From Equation (46) we have

$$\alpha A s \tilde{f}(s) = I[1 + s\tilde{\kappa}(s)], \quad (70)$$

and this gives

$$\tilde{P}_0(s) = \frac{1 + I\tilde{\kappa}(s)}{s + I[1 + s\tilde{\kappa}(s)]}. \quad (71)$$

Here, $\tilde{\kappa}(0)$ is finite, so we find

$$\tilde{P}_0(0) = \frac{1}{I} + \delta_{m0}\tilde{\kappa}(0). \quad (72)$$

Therefore, the average waiting time for the n th photon is

$$\langle\tau_n\rangle = \frac{n}{I} + \tilde{\kappa}(0). \quad (73)$$

For random events, this would be $\langle\tau_n\rangle = n/I$, so the term $\tilde{\kappa}(0)$ accounts for the effect of the correlations between the photons on the waiting time. With Equation (15) this becomes

$$\langle\tau_n\rangle = \frac{1}{2I}[2n + Q(\infty)], \quad (74)$$

so the deviation from Poisson statistics can be expressed in terms of the Q factor for infinite counting time. For $Q(\infty) < 0$, the average waiting time is smaller than for random events, and $Q(\infty) \geq -1$ sets a lower bound on the waiting time.

The variance of τ_n can be obtained along similar lines, but the computation is much more involved. The result is

$$(\Delta\tau_n)^2 = \frac{n}{I^2} + \left(\frac{2n}{I} + \tilde{\kappa}(0)\right)\tilde{\kappa}(0) - 2\tilde{\kappa}'(0). \quad (75)$$

For Poisson statistics this would be n/I^2 . This result involves the derivative of $\tilde{\kappa}(s)$, which can be found from Equation (49). An interesting case is $\Delta^2 = 3A^2/4$,

for which $Q(\infty) = 0$. Then the long-time counting statistics is Poisson, and $\langle\tau_n\rangle$ is the same as for Poisson statistics. The variance, however, is

$$(\Delta\tau_n)^2 = \frac{n}{I^2} + \frac{8}{2A^2 + \Omega_0^2}, \quad (76)$$

and this is larger than for independent events.

The conditional probability for the detection of the n th photon is $w_n(t|0)$, and the Laplace transform of this function is given by Equation (67). We see immediately that $\tilde{w}_n(0|0) = 0$, so the condition in Equation (30) is satisfied. In order to find the conditional waiting time, we proceed as above. For $w_n(t|0)$ we use the representation of Equation (27), and integrate by parts. Instead of $\tilde{P}_m(0)$ in Equation (69), we now get $\tilde{w}_m(0)$, and $\tilde{w}_m(0) = 1$. Therefore

$$\langle\tau_n|0\rangle = \frac{n}{I}, \quad (77)$$

and there are no correlation effects in this average waiting time. The variance becomes

$$(\Delta\tau_n|0)^2 = \frac{n}{I^2} + \frac{2n}{I}\tilde{\kappa}(0), \quad (78)$$

and this is also

$$(\Delta\tau_n|0)^2 = \frac{n}{I^2}[1 + Q(\infty)]. \quad (79)$$

Apparently, for the conditional waiting times the variance deviates from its Poisson value, rather than the average, and this deviation can be expressed in terms of $Q(\infty)$. The results in Equations (74) and (75) were found before [18], although the variance was expressed in a different form, and Equations (78) and (79) generalize the result of [19], where the case $n = 1$ was considered.

The Q factor for long counting times, $Q(\infty)$, can be experimentally determined by measuring $\sigma(T)^2$ (and $\mu(T) = IT$), according to its definition in Equation (8). Alternatively, measurement of the two-photon correlation function $I_2(0, \tau)$ yields $Q(\infty)$ with Equation (13). From the above we see that $Q(\infty)$ can also be found from the average waiting time for the first photon, with Equation (74), or the standard deviation in the conditional waiting time for the first photon, Equation (79). From Equations (15) and (72) we find

$$Q(\infty) = -2 + 2I \int_0^\infty dTP_0(T). \quad (80)$$

This shows that $Q(\infty)$ can also be obtained from the T dependence of the probability of finding zero photons in $[0, T]$.

8. Conditional probability densities

The Laplace transform of the conditional probability density $w_n(t|0)$ for the detection of the n th photon is given by Equation (67). We notice that

$$\tilde{w}_{n+1}(s|0) = \tilde{w}_n(s|0)\tilde{w}_1(s|0), \quad (81)$$

and therefore

$$w_n(t|0) = \int_0^t d\tau w_{n-1}(\tau|0)w_1(t-\tau|0), \quad n = 2, 3, \dots \quad (82)$$

Consequently, all probability densities $w_n(t|0)$ can be found successively by integration as soon as $w_1(t|0)$ is known. The Laplace transform of $w_1(t|0)$ is

$$\begin{aligned} \tilde{w}_1(s|0) &= \frac{1}{2}\alpha A\Omega_0^2 \left(\frac{1}{2}A + s \right) \\ &\times \left\{ s(A+s) \left[\left(\frac{1}{2}A + s \right)^2 + \Delta^2 \right] \right. \\ &\left. + \left(\frac{1}{2}A + s \right) \left(\frac{1}{2}\alpha A + s \right) \Omega_0^2 \right\}^{-1}. \end{aligned} \quad (83)$$

For the computation of the Laplace inverse, we would need to factor a 4th degree polynomial. The parameter α has the significance of the detection probability of an emitted photon. We shall now consider the case $\alpha = 1$, so this refers to the emission statistics of the photons, rather than the detection statistics. In addition, we shall consider resonance, so $\Delta = 0$. Then we easily find

$$w_1(t|0) = A \frac{2\hat{\Omega}_0^2}{\rho_3^2} \left[\cosh\left(\frac{1}{2}\rho_3 \hat{t}\right) - 1 \right] e^{-\frac{1}{2}\hat{t}}, \quad (84)$$

with

$$\rho_3 = \sqrt{1 - 4\hat{\Omega}_0^2}. \quad (85)$$

For $\hat{\Omega}_0 = 1/2$, the right-hand side of Equation (84) should be considered with a limit, and the result is

$$w_1(t|0) = \frac{1}{4} A \hat{\Omega}_0^2 \hat{t}^2 e^{-\frac{1}{2}\hat{t}}. \quad (86)$$

Figure 8 shows $w_1(t|0)$ for two values of $\hat{\Omega}_0$. For small values of $\hat{\Omega}_0$, the curve has a single peak, but for large $\hat{\Omega}_0$ oscillations appear. The average and the standard deviation are with Equations (77), (79) and (51)

$$A\langle\tau_1|0\rangle = \frac{1 + 2\hat{\Omega}_0^2}{\hat{\Omega}_0^2}, \quad (87)$$

$$A(\Delta\tau_1|0) = \frac{1}{\hat{\Omega}_0^2} \sqrt{4\hat{\Omega}_0^4 - 2\hat{\Omega}_0^2 + 1}. \quad (88)$$

Both functions are shown in Figure 9. The average decreases monotonically with $\hat{\Omega}_0$, but the standard deviation has a shallow minimum of $\sqrt{3}$ for $\hat{\Omega}_0 = 1$.

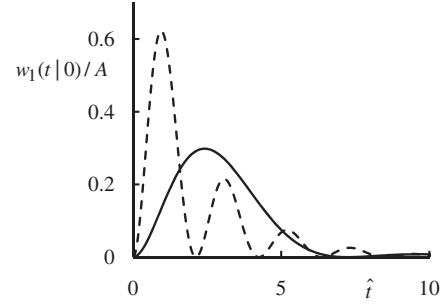


Figure 8. Graphs of $w_1(t|0)/A$ for $\Delta = 0$ and $\alpha = 1$. For the dashed and solid curves we have $\hat{\Omega}_0 = 3$ and $\hat{\Omega}_0 = 1$, respectively. For smaller values of $\hat{\Omega}_0$ the peak moves to the right and the curve flattens.

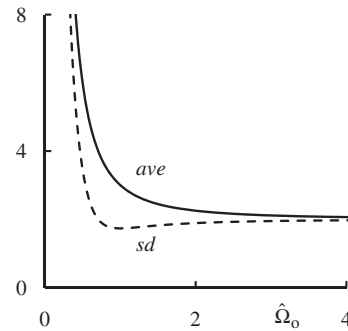


Figure 9. The average (solid curve) and standard deviation (dashed curve) for τ_1 as a function of $\hat{\Omega}_0$. The standard deviation has a minimum at $\hat{\Omega}_0 = 1$.

It is interesting to note that the minimum of $Q(\infty)$ for $\hat{\Delta} = 0$ appears at $\hat{\Omega}_0 = 1/\sqrt{2}$. At this value, the standard deviation is 2. For high laser power, both the average and the standard deviation approach the limit of 2.

With Equation (82) we can now find $w_n(t|0)$ for $n = 2, 3, \dots$. The first few are

$$\begin{aligned} w_2(t|0) &= A \left(\frac{2\hat{\Omega}_0^2}{\rho_3^2} \right)^2 \left\{ \hat{t} \left[1 + \frac{1}{2} \cosh\left(\frac{1}{2}\rho_3 \hat{t}\right) \right] \right. \\ &\quad \left. - \frac{3}{\rho_3} \sinh\left(\frac{1}{2}\rho_3 \hat{t}\right) \right\} e^{-\frac{1}{2}\hat{t}}, \end{aligned} \quad (89)$$

$$\begin{aligned} w_3(t|0) &= A \left(\frac{2\hat{\Omega}_0^2}{\rho_3^2} \right)^3 \left\{ \frac{\hat{t}}{8} \left[\cosh\left(\frac{1}{2}\rho_3 \hat{t}\right) - 4 \right] \right. \\ &\quad \left. + \frac{12}{\rho_3^2} \left[\cosh\left(\frac{1}{2}\rho_3 \hat{t}\right) - 1 \right] - \frac{9\hat{t}}{4\rho_3} \sinh\left(\frac{1}{2}\rho_3 \hat{t}\right) \right\} e^{-\frac{1}{2}\hat{t}}. \end{aligned} \quad (90)$$

For the average and the standard deviation of τ_n we have

$$\langle\tau_n|0\rangle = n\langle\tau_1|0\rangle, \quad (91)$$

$$(\Delta\tau_n|0) = \sqrt{n}(\Delta\tau_1|0), \quad (92)$$

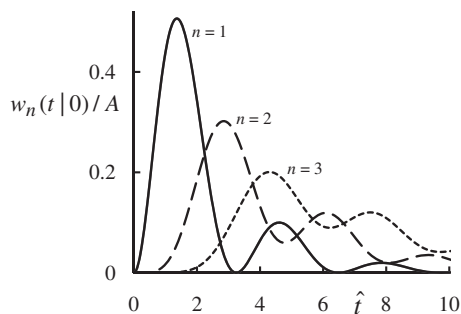


Figure 10. Graphs of $w_n(t|0)$ for $n=1, 2$ and 3 , and for $\hat{\Omega}_0 = 2$. The corresponding averages are $9n/4$.

and therefore the behavior is the same as in Figure 9. In particular, the standard deviation is minimum at $\hat{\Omega}_0 = 1$ for all n . Figure 10 shows $w_n(t|0)$ for $n=1, 2$ and 3 , and with $\hat{\Omega}_0 = 2$. We notice the long tails for large \hat{t} , and we see that for this value of $\hat{\Omega}_0$ there is not a clear peak near the average (as there is for smaller $\hat{\Omega}_0$).

9. Probability densities

The probability densities can be found from the conditional probability densities with Equations (28) and (29), and $w_n(0) = I\delta_{n1}$ for resonance fluorescence. For $n=1$ we obtain

$$w_1(t) = Ie^{-\frac{1}{2}\hat{t}} \left\{ 1 + \frac{1}{\rho_3} \left[\sinh\left(\frac{1}{2}\rho_3\hat{t}\right) + \frac{1}{\rho_3} \left[\cosh\left(\frac{1}{2}\rho_3\hat{t}\right) - 1 \right] \right] \right\}, \quad (93)$$

and the intensity is

$$I = A \frac{\hat{\Omega}_0^2}{1 + 2\hat{\Omega}_0^2}. \quad (94)$$

Although Equation (93) may seem similar in appearance as Equation (84) for the conditional probability, the properties of $w_1(t)$ are quite different. Figure 11 shows graphs of $w_1(t)$ for various values of $\hat{\Omega}_0$. The first difference with the conditional probability $w_1(t|0)$ is that $w_1(0) = I$, rather than zero. As compared to Figure 8 for the conditional probabilities, we also notice that the probabilities in Figure 11 do not nearly oscillate as much. In fact, in Figure 8 the number of oscillations increases with $\hat{\Omega}_0$, whereas in Figure 11 they seem to smoothen out for large $\hat{\Omega}_0$. We see from Equations (93) and (94) that for $\hat{\Omega}_0$ large the probability density approaches the limit

$$w_1(t) = \frac{1}{2}Ae^{-\frac{1}{2}\hat{t}}, \quad (\hat{\Omega}_0 \rightarrow \infty), \quad (95)$$

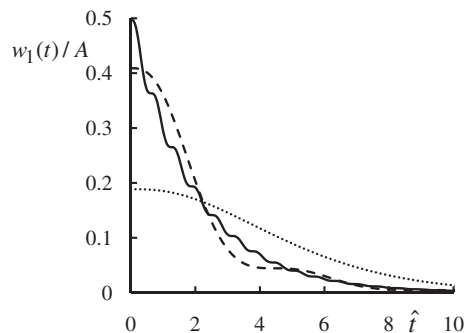


Figure 11. Graphs of $w_1(t)$ for $\hat{\Omega}_0 = 0.55$ (dotted curve), $\hat{\Omega}_0 = 1.5$ (dashed curve) and $\hat{\Omega}_0 = 10$ (solid curve). The solid curve is very close to its high-intensity limit, given by Equation (95).

whereas in Figure 8 the oscillations persist for large $\hat{\Omega}_0$.

The average waiting time for the first photon is with Equation (73)

$$A\langle\tau_1\rangle = \frac{4\hat{\Omega}_0^4 + \hat{\Omega}_0^2 + 1}{\hat{\Omega}_0^2(2\hat{\Omega}_0^2 + 1)}. \quad (96)$$

The behavior is very similar as for $A\langle\tau_1|0\rangle$ in Figure 9. For $\hat{\Omega}_0$ small, the waiting time $A\langle\tau_1\rangle$ is very large, and for $\hat{\Omega}_0 \rightarrow \infty$ we have $A\langle\tau_1|0\rangle \rightarrow 2$, which is twice the lifetime of the excited state. This comes from the fact that the population of the excited state is $\bar{n}_e = 1/2$ for $\hat{\Omega}_0 \rightarrow \infty$. The right-hand side of Equation (96) has a very shallow minimum of 1.90 at $\hat{\Omega}_0^2 = 1 + \sqrt{3}/2$.

For $n=2$ we find with Equation (29) and the results from the previous section

$$w_2(t) = I \left(\frac{2\hat{\Omega}_0^2}{\rho_3^4} \right) e^{-\frac{1}{2}\hat{t}} \left[2 + 4\hat{\Omega}_0^2\hat{t} + \left(2\rho_3 - \frac{3}{\rho_3} + \frac{1}{2}\rho_3\hat{t} \right) \times \sinh\left(\frac{1}{2}\rho_3\hat{t}\right) + \left(\frac{1}{2}\hat{t} - 2 \right) \cosh\left(\frac{1}{2}\rho_3\hat{t}\right) \right]. \quad (97)$$

In the strong field limit, this becomes

$$w_2(t) = \frac{1}{4}A\hat{t}e^{-\frac{1}{2}\hat{t}}, \quad (\hat{\Omega}_0 \rightarrow \infty). \quad (98)$$

Figure 12 shows $w_n(t)$ for $n=1$ and 2 , and for $\hat{\Omega}_0 = 2$.

10. Probabilities

Once the probability densities $w_n(t)$ are known, the probabilities $P_n(T)$ for the detection of n photons in $[0, T]$ can be obtained from Equations (18) and (19). We thus obtain

$$P_0(T) = \frac{1}{2\rho_3^2} \frac{1}{1 + 2\hat{\Omega}_0^2} e^{-\frac{1}{2}\hat{T}} \left[(\rho_3^2 + 1) \cosh\left(\frac{1}{2}\rho_3\hat{T}\right) + 2\rho_3 \sinh\left(\frac{1}{2}\rho_3\hat{T}\right) - 16\hat{\Omega}_0^4 \right], \quad (99)$$

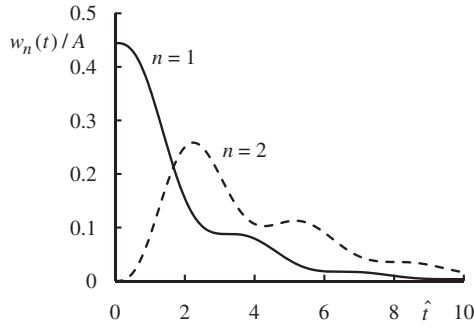


Figure 12. Graphs of $w_1(t)$ (solid curve) and $w_2(t)$ (dashed curve) for $\hat{\Omega}_o = 2$.

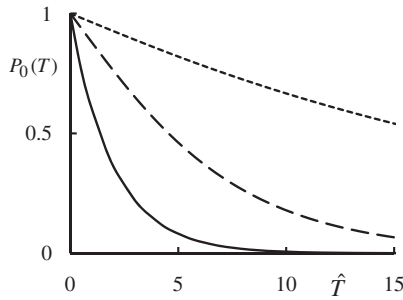


Figure 13. Graphs of $P_0(T)$, given by Equation (99), for $\hat{\Omega}_o = 0.2$ (dotted line), 0.4 (dashed line) and 5 (solid line). The solid curve is indistinguishable from the high-intensity limit of Equation (101).

$$P_1(T) = \frac{\hat{\Omega}_o^2}{\rho_3^4} \frac{1}{1 + 2\hat{\Omega}_o^2} e^{-\frac{1}{2}\hat{T}} \left\{ 4\hat{\Omega}_o^2 \left\{ 4 \left[1 - \cosh\left(\frac{1}{2}\rho_3 \hat{T}\right) \right] - \frac{3}{\rho_3} \sinh\left(\frac{1}{2}\rho_3 \hat{T}\right) \right\} + \frac{1}{2}\hat{T} \left\{ 32\hat{\Omega}_o^4 + (\rho_3^2 + 1) \times \cosh\left(\frac{1}{2}\rho_3 \hat{T}\right) + 2\rho_3 \sinh\left(\frac{1}{2}\rho_3 \hat{T}\right) \right\} \right\}. \quad (100)$$

Figures 13 and 14 show graphs of $P_0(T)$ and $P_1(T)$, respectively, for various values of $\hat{\Omega}_o$. In the high intensity limit $\hat{\Omega}_o \rightarrow \infty$ we find

$$P_0(T) = e^{-\frac{1}{2}\hat{T}}, \quad (101)$$

$$P_1(T) = \frac{1}{2}\hat{T}e^{-\frac{1}{2}\hat{T}}. \quad (102)$$

The probabilities for larger values of n can be obtained similarly, but obviously with increasing effort.

11. Conclusions

Resonant fluorescent photons are correlated, and this is reflected in the counting statistics. The Q factor is a measure for the deviation of the counting statistics

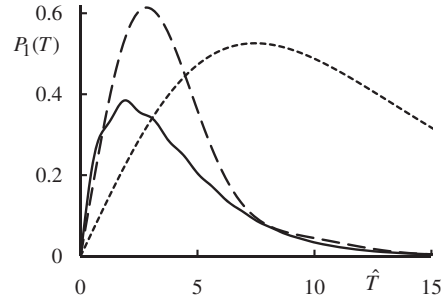


Figure 14. Graphs of $P_1(T)$, given by Equation (100), for $\hat{\Omega}_o = 0.4$ (dotted line), 1 (dashed line) and 5 (solid line). The solid curve is close to the high-intensity limit of Equation (102), although some wiggles are still present for this value of $\hat{\Omega}_o$.

from Poisson statistics. For small counting times T , $Q(T)$ is negative as a result of the antibunching of the emitted photons. For longer counting times, $Q(T)$ can become positive, and consequently there exists a point T_P , a Poisson point, where the variance of the count distribution equals the average. We have shown by example that there is one such point when $Q(\infty) > 0$, and none otherwise.

We have considered the probability density $w_n(t)$ for the detection on the n th photon, and the conditional probability $w_n(t|0)$ for the detection of the n th photon, after a detection of a photon at time zero. In the Appendix, general relations for these functions are derived. It is shown that for resonance fluorescence these functions can be computed recursively as soon as $w_1(t|0)$ is known. We have computed explicitly the function $w_n(t|0)$ for $n = 1, 2$ and 3 for the case of resonance and where all emitted photons are detected ($\alpha = 1$), and the function $w_n(t)$ for $n = 1$ and 2 for the same case. It is shown that the probabilities $P_n(T)$ for the emission of n photons in the time interval $[0, T]$ can be found from the probability densities, and we have illustrated this by computing $P_0(T)$ and $P_1(T)$.

References

- [1] van Kampen, N.G. *Stochastic Processes in Physics and Chemistry*, 3rd ed.; Elsevier: Amsterdam, 2007, Chapter 2.
- [2] Stratonovich, R.L. *Topics in the Theory of Random Noise*; Gordon and Breach: New York, 1963; Vol. 1, Chapter 6.
- [3] Glauber, R.J. In *Quantum Optics and Electronics*; DeWitt, C., Blandin, A., Cohen-Tannoudji, C., Eds.; Gordon and Breach: New York, 1965; pp 65–185.
- [4] Kelley, P.L.; Kleiner, W.H. *Phys. Rev.* **1964**, *136*, A316–A334.
- [5] Kimble, H.J.; Dagenais, M.; Mandel, L. *Phys. Rev. Lett.* **1977**, *39*, 691–695.

[6] Dagenais, M.; Mandel, L. *Phys. Rev. A: At., Mol., Opt. Phys.* **1978**, *18*, 2217–2228.
 [7] Diedrich, F.; Walther, H. *Phys. Rev. Lett.* **1987**, *58*, 203–206.
 [8] Loudon, R. *Rep. Prog. Phys.* **1980**, *43*, 913–949.
 [9] Mandel, L.; Wolf, E. *Optical Coherence and Quantum Optics*; Cambridge University Press: New York, 1995; p 450.
 [10] Short, R.; Mandel, L. *Phys. Rev. Lett.* **1983**, *51*, 384–387.
 [11] Hodapp, T.W.; Greenless, G.W.; Finn, M.A.; Lewis, D.A. *Phys. Rev. A: At., Mol., Opt. Phys.* **1990**, *41*, 2698–2701.
 [12] Oldaker, B.G.; Martin, P.J.; Gould, P.L.; Xiao, M.; Pritchard, D.E. *Phys. Rev. Lett.* **1990**, *65*, 1555–1558.
 [13] Hoogerland, M.D.; Wijnands, M.N.J.H.; Senhorst, H.A.J.; Beijerinck, H.C.W.; Leeuwen, K.A.H. *Phys. Rev. Lett.* **1990**, *65*, 1559–1562.
 [14] Hodapp, T.W.; Finn, M.A.; Greenless, G.W. *Phys. Rev. A: At., Mol., Opt. Phys.* **1992**, *46*, 4234–4238.
 [15] Agarwal, G.S. *Phys. Rev. A: At., Mol., Opt. Phys.* **1977**, *15*, 814–816.
 [16] Lenstra, D. *Phys. Rev. A: At., Mol., Opt. Phys.* **1982**, *26*, 3369–3377.
 [17] Walls, D.F.; Milburn, G.J. *Quantum Optics*; Berlin: Springer, 1994; p 221.
 [18] Arnoldus, H.F.; Nienhuis, G. *Opt. Acta* **1983**, *30*, 1573–1585.
 [19] Arnoldus, H.F.; Nienhuis, G. *Opt. Acta* **1986**, *33*, 691–702.
 [20] Carmichael, H.J.; Singh, S.; Vyas, R.; Rice, P.R. *Phys. Rev. A: At., Mol., Opt. Phys.* **1989**, *39*, 1200–1218.

Appendix

In this Appendix we shall derive the various relations for the probability densities and the conditional probability densities. Let $P_n(t)$ be the probability for n events in $[0, t]$. Here we write t , rather than T , since for the probability densities the counting time is a running variable. The derivation of the various relations is facilitated by the use of diagrams. Figure 15 shows the definitions of $P_n(t)$ and $w_n(t)$. Then we consider $P_n(t + dt)$, as shown in Figure 16. The probability for zero events in $[0, t + dt]$ is the same as the probability for zero events in $[0, t]$ and also no events in $[t, t + dt]$, as illustrated in the top diagram. For $n \geq 1$, however, there are two ways in which we can have n events in $[0, t + dt]$, as shown in the lower diagram. Since both outcomes are

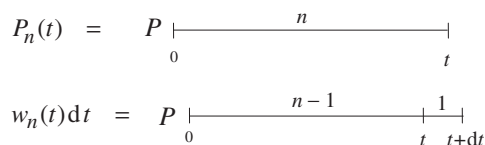


Figure 15. Schematic illustration of the definitions of $P_n(t)$ and $w_n(t)$.

exclusive, the probabilities add. Then, as shown in Figure 17, we can view $P_n(t)$, the left-hand side, as the sum of two contributions, since there can only be zero or one event in $[t, t + dt]$. Then we use the relation from Figure 17 to eliminate the first terms on the right-hand sides of both diagrams in Figure 16, which yields the relations depicted in Figure 18. In the diagrams in Figure 18, each term can be expressed with a $P_n(t)$ or a $w_n(t)$, and we obtain

$$P_0(t + dt) = P_0(t) - w_1(t)dt, \tag{A1}$$

$$P_n(t + dt) = P_n(t) - w_{n+1}(t)dt + w_n(t)dt, \quad n = 1, 2, \dots \tag{A2}$$

This is

$$\frac{d}{dt}P_0(t) = -w_1(t), \tag{A3}$$

$$\frac{d}{dt}P_n(t) = -w_{n+1}(t) + w_n(t), \quad n = 1, 2, \dots, \tag{A4}$$

with solution

$$w_n(t) = -\frac{d}{dt} \sum_{m=0}^{n-1} P_m(t). \tag{A5}$$

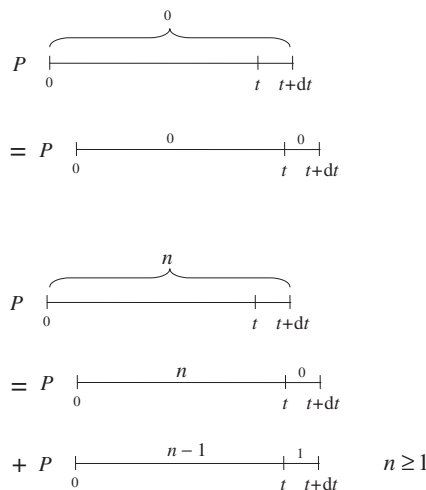


Figure 16. Equalities for $P_n(t + dt)$. For $n = 0$, there is only one term (top diagram), but for $n > 0$ there are two possibilities (lower diagram).

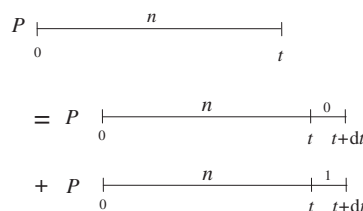


Figure 17. The figure shows that $P_n(t)$ can be written as the sum of two terms.

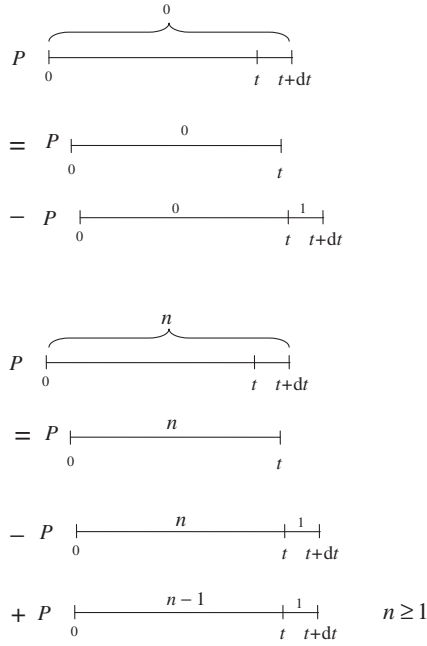


Figure 18. Combinations of previous diagrams that lead to Equations (A1) and (A2) for the probability densities.

$$w_n(t_a, t_b) dt_b = P \left| \begin{array}{c} \text{---} \overbrace{\text{---}}^{n-1} \text{---} \\ t_a \qquad \qquad \qquad t_b \quad t_b + dt_b \end{array} \right|$$

$$w_n(t_a, t_b | t_a) I(t_a) dt_a dt_b = P \left| \begin{array}{c} \text{---} \overbrace{\text{---}}^{n-1} \text{---} \\ t_a - dt_a \quad t_a \qquad \qquad \qquad t_b \quad t_b + dt_b \end{array} \right|$$

Figure 19. The definitions of $w_n(t_a, t_b)$ and $w_n(t_a, t_b | t_a)$.

We now consider the conditional probability densities. To this end, we first rename the initial time as t_a , rather than $t = 0$, and we set $t_b = t$. Then the probability densities are $w_n(t_a, t_b)$, in obvious notation. The conditional probability densities are defined as

$$w_n(t_a, t_b | t_a) dt_b = \text{probability that the } n\text{th event is in } [t_b, t_b + dt_b] \text{ after an event in } [t_a - dt_a, t_a], \tag{A6}$$

for $n = 1, 2, \dots$. If the functions $P_n(t)$ are known, then the average $\mu(t)$ is given by Equation (6). Then

$$I(t) = \frac{d}{dt} \mu(t), \tag{A7}$$

which defines the intensity of the random process (we set $I_1(t) = I(t)$). With Equation (1) we then have that $I(t)dt$ equals the probability for an event in $[t, t + dt]$, irrespective of events at other times. Figure 19 shows

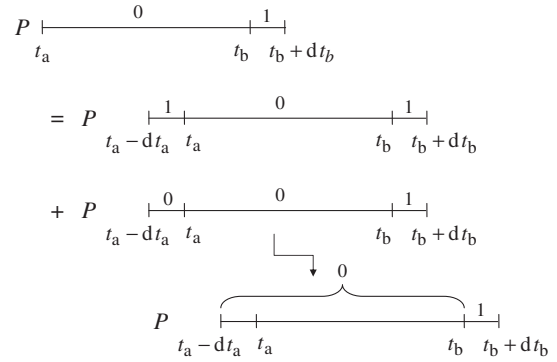


Figure 20. The figure shows that $w_1(t_a, t_b)dt_b$ can be written as the sum of two terms. This leads to Equation (A9).

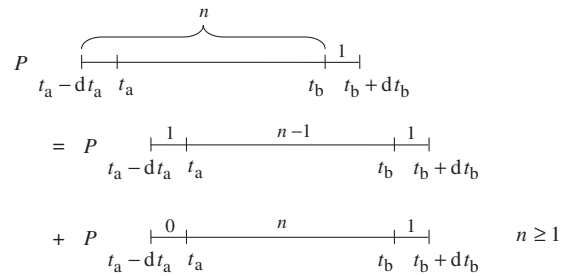


Figure 21. The diagram shows a relation for $w_{n+1}(t_a - dt_a, t_b)dt_b$.

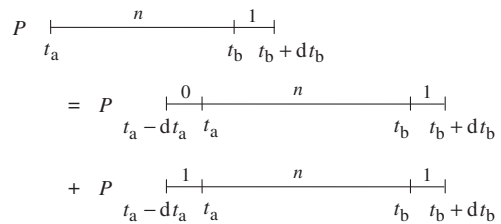


Figure 22. The diagram shows a relation for $w_{n+1}(t_a, t_b)dt_b$.

schematically $w_n(t_a, t_b)dt_b$ and $w_n(t_a, t_b | t_a)I(t_a)dt_a dt_b$. For $n = 1$ we have

$$w_1(t_a, t_b)dt_b = w_1(t_a, t_b | t_a)I(t_a)dt_a dt_b + w_1(t_a - dt_a, t_b)dt_b, \tag{A8}$$

as follows from the diagram in Figure 20. This is

$$w_1(t_a, t_b | t_a) = \frac{1}{I(t_a)} \frac{\partial}{\partial t_a} w_1(t_a, t_b). \tag{A9}$$

Then we consider $w_{n+1}(t_a - dt_a, t_b)dt_b$ the diagram for which is on the left-hand side of the equation in Figure 21. The second term on the right-hand side is eliminated with the identity in Figure 22, and this gives the relation shown in Figure 23. This yields the relation

$$w_{n+1}(t_a - dt_a, t_b)dt_b = w_n(t_a, t_b | t_a)I(t_a)dt_a dt_b + w_{n+1}(t_a, t_b)dt_b - w_{n+1}(t_a, t_b | t_a)I(t_a)dt_a dt_b, \tag{A10}$$

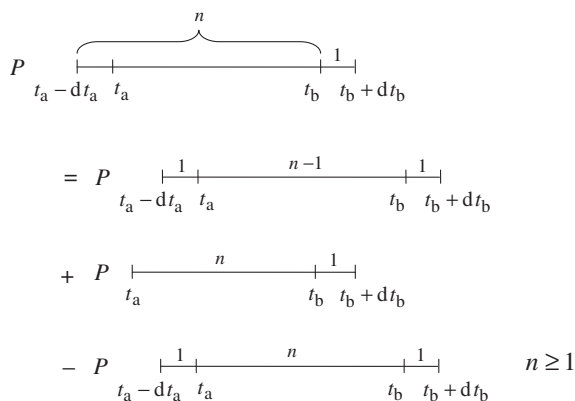


Figure 23. This diagram is a combination of previous ones, and leads to Equation (A10).

and this is

$$\frac{\partial}{\partial t_a} w_{n+1}(t_a, t_b) = I(t_a)[w_{n+1}(t_a, t_b|t_a) - w_n(t_a, t_b|t_a)], \quad n = 1, 2, \dots \quad (A11)$$

Solving by iteration gives

$$w_n(t_a, t_b|t_a) = \frac{1}{I(t_a)} \frac{\partial}{\partial t_a} \sum_{m=1}^n w_m(t_a, t_b), \quad (A12)$$

and for $n = 1$ this is Equation (A9).

The conditional probabilities $P_n(t_a, t_b|t_a)$ are defined as

$$P_n(t_a, t_b|t_a) = \text{probability for } n \text{ events in } [t_a, t_b] \text{ after an event in } [t_a - dt_a, t_a], \quad (A13)$$

and the diagram is shown in Figure 24. Along similar lines as above, we obtain

$$\frac{\partial}{\partial t_a} P_0(t_a, t_b) = I(t_a)P_0(t_a, t_b|t_a), \quad (A14)$$

$$\frac{\partial}{\partial t_a} P_n(t_a, t_b) = I(t_a)[P_n(t_a, t_b|t_a) - P_{n-1}(t_a, t_b|t_a)], \quad n = 1, 2, \dots, \quad (A15)$$

$$P_n(t_a, t_b|t_a)I(t_a)dt_a = P \begin{array}{c} | \quad | \quad | \quad | \\ t_a - dt_a \quad t_a \quad t_b \quad t_b + dt_b \end{array} \quad (A16)$$

Figure 24. The definition of the conditional probability $P_n(t_a, t_b|t_a)$.

$$I dt P_n(t|0) = P \begin{array}{c} | \quad | \quad | \quad | \\ -dt \quad 0 \quad t \end{array} \quad (A17)$$

$$w_{n+1}(t)dt = P \begin{array}{c} | \quad | \quad | \quad | \\ 0 \quad t \quad t+dt \end{array} \quad (A18)$$

Figure 25. Two diagrams for which the probabilities are equal for a stationary process.

by considering several diagrams. The solution is

$$P_n(t_a, t_b|t_a) = \frac{1}{I(t_a)} \frac{\partial}{\partial t_a} \sum_{m=0}^n P_m(t_a, t_b). \quad (A16)$$

For a stationary process we have $w_n(t_a, t_b) = w_n(0, t_b - t_a)$ and $w_n(t_a, t_b|t_a) = w_n(0, t_b - t_a|0)$. We set $t = t_b - t_a$, and write $w_n(t)$ and $w_n(t|0)$, respectively. With $\partial/\partial t_a \rightarrow -d/dt$, Equation (A12) becomes

$$w_n(t|0) = -\frac{1}{I} \frac{d}{dt} \sum_{m=1}^n w_m(t). \quad (A17)$$

For a stationary process, Equation (A16) becomes

$$P_n(t|0) = -\frac{1}{I} \frac{d}{dt} \sum_{m=0}^n P_m(t). \quad (A18)$$

Comparison with Equation (A5) shows

$$w_{n+1}(t) = IP_n(t|0), \quad (A19)$$

so for a stationary process the probabilities $I dt P_n(t|0)$ and $w_{n+1}(t)dt$ are equal. The diagrams for both probabilities are shown in Figure 25. Apparently, a conditional event before or after the n events in $[0, t]$ has the same effect for a stationary process.